Disappearance of Back-To-Back High-p_T Hadron Correlations in Central Au + Au Collisions at $\sqrt{s_{NN}} = 200$ GeV

C. Adler,[11] Z. Ahammed,[23] C. Allgower,[12] J. Amonett,[14] B. D. Anderson,[14] M. Anderson,[5] G. S. Averichev,[9]
J. Balewski,[12] O. Barannikova,[9,23] L. S. Barnby,[14] J. Baudot,[13] S. Bekele,[20] V.V. Belaga,[9] R. Bellwied,[31] J. Berger,[11]
H. Bichsel,[30] A. Billmeier,[31] L. C. Bland,[2] C. O. Blyth,[3] B. E. Bonner,[24] A. Boucham,[26] A. Brandin,[18] A. Bravar,[2]
R.V. Cadman,[1] H. Caines,[33] M. Calderón de la Barca Sánchez,[2] A. Cardenas,[23] J. Carroll,[15] J. Castillo,[26] M. Castro,[31]
D. Cebra,[5] P. Chaloupka,[20] S. Chattopadhyay,[31] Y. Chen,[6] S. P. Chernenko,[9] M. Cherney,[8] A. Chikanian,[33] B. Choi,[28]
W. Christie,[2] J. P. Coffin,[13] T. M. Cormier,[31] M. M. Corral,[16] J. G. Cramer,[30] H. J. Crawford,[4] A. A. Derevschikov,[22]
L. Didenko,[2] T. Dietel,[11] J. E. Draper,[5] V. B. Dunin,[9] J. C. Dunlop,[33] V. Eckardt,[16] L. G. Efimov,[9] V. Emelianov,[18]
J. Engelage,[4] G. Eppley,[24] B. Erazmus,[26] P. Fachini,[2] V. Faine,[2] J. Faivre,[13] R. Fatemi,[12] K. Filimonov,[15] E. Finch,[33]
Y. Fisyak,[2] D. Flierl,[11] K. J. Foley,[2] J. Fu,[15,32] C. A. Gagliardi,[27] N. Gagunashvili,[9] J. Gans,[33] L. Gaudichet,[26]
M. Germain,[13] F. Geurts,[24] V. Ghazikhanian,[6] O. Grachov,[31] V. Grigoriev,[18] M. Guedon,[13] E. Gushin,[18] T. J. Hallman,[2]
D. Hardtke,[15] J.W. Harris,[33] T.W. Henry,[27] S. Heppelmann,[21] T. Herston,[23] B. Hippolyte,[13] A. Hirsch,[23] E. Hjort,[15]
G.W. Hoffmann,[28] M. Horsley,[33] H. Z. Huang,[6] T. J. Humanic,[20] G. Igo,[6] A. Ishihara,[28] Yu. I. Ivanshin,[10] P. Jacobs,[15]
W.W. Jacobs,[12] M. Janik,[29] I. Johnson,[15] P. G. Jones,[3] E. G. Judd,[4] M. Kaneta,[15] M. Kaplan,[7] D. Keane,[14] J. Kiryluk,[6]
A. Kisiel,[29] J. Klay,[15] S. R. Klein,[15] A. Klyachko,[12] T. Kollegger,[11] A. S. Konstantinov,[22] M. Kopytine,[14] L. Kotchenda,[18]
A. D. Kovalenko,[9] M. Kramer,[19] P. Kravtsov,[18] K. Krueger,[1] C. Kuhn,[13] A. I. Kulikov,[9] G. J. Kunde,[33] C. L. Kunz,[7]
R. Kh. Kutuev,[10] A. A. Kuznetsov,[9] L. Lakehal-Ayat,[26] M. A. C. Lamont,[3] J. M. Landgraf,[2] S. Lange,[11] C. P. Lansdell,[28]
B. Lasiuk,[33] F. Laue,[2] J. Lauret,[2] A. Lebedev,[2] R. Lednický,[9] V. M. Leontiev,[22] M. J. LeVine,[2] Q. Li,[31]
S. J. Lindenbaum,[19] M. A. Lisa,[20] F. Liu,[32] L. Liu,[32] Z. Liu,[32] Q. J. Liu,[30] T. Ljubicic,[2] W. J. Llope,[24] G. LoCurto,[16]
H. Long,[6] R. S. Longacre,[2] M. Lopez-Noriega,[20] W. A. Love,[2] T. Ludlam,[2] D. Lynn,[2] J. Ma,[6] D. Magestro,[20] R. Majka,[33]
S. Margetis,[14] C. Markert,[33] L. Martin,[26] J. Marx,[15] H. S. Matis,[15] Yu. A. Matulenko,[22] T. S. McShane,[8] F. Meissner,[15]
Yu. Melnick,[22] A. Meschanin,[22] M. Messer,[2] M. L. Miller,[33] Z. Milosevich,[7] N. G. Minaev,[22] J. Mitchell,[24]
C. F. Moore,[28] V. Morozov,[15] M. M. de Moura,[31] M. G. Munhoz,[25] J. M. Nelson,[3] P. Nevski,[2] V. A. Nikitin,[10]
L.V. Nogach,[22] B. Norman,[14] S. B. Nurushev,[22] G. Odyniec,[15] A. Ogawa,[21] V. Okorokov,[18] M. Oldenburg,[16] D. Olson,[15]
G. Paic,[20] S. U. Pandey,[31] Y. Panebratsev,[9] S. Y. Panitkin,[2] A. I. Pavlinov,[31] T. Pawlak,[29] V. Perevoztchikov,[2] W. Peryt,[29]
V. A Petrov,[10] M. Planinic,[12] J. Pluta,[29] N. Porile,[23] J. Porter,[2] A. M. Poskanzer,[15] E. Potrebenikova,[9] D. Prindle,[30]
C. Pruneau,[31] J. Putschke,[16] G. Rai,[15] G. Rakness,[12] O. Ravel,[26] R. L. Ray,[28] S.V. Razin,[9,12] D. Reichhold,[8] J. G. Reid,[30]
G. Renault,[26] F. Retiere,[15] A. Ridiger,[18] H. G. Ritter,[15] J. B. Roberts,[24] O.V. Rogachevski,[9] J. L. Romero,[5] A. Rose,[31]
C. Roy,[26] V. Rykov,[31] I. Sakrejda,[15] S. Salur,[33] J. Sandweiss,[33] I. Savin,[10] J. Schambach,[28] R. P. Scharenberg,[23]
N. Schmitz,[16] L. S. Schroeder,[15] A. Schüttauf,[16] K. Schweda,[15] J. Seger,[8] D. Seliverstov,[18] P. Seyboth,[16] E. Shahaliev,[9]
K. E. Shestermanov,[22] S. S. Shimanskii,[9] F. Simon,[16] G. Skoro,[9] N. Smirnov,[33] R. Snellings,[15] P. Sorensen,[6] J. Sowinski,[12]
H. M. Spinka,[1] B. Srivastava,[23] E. J. Stephenson,[12] R. Stock,[11] A. Stolpovsky,[31] M. Strikhanov,[18] B. Stringfellow,[23]
C. Struck,[11] A. A. P. Suaide,[31] E. Sugarbaker,[20] C. Suire,[2] M. Šumbera,[20] B. Surrow,[2] T. J. M. Symons,[15]
A. Szanto de Toledo,[25] P. Szarwas,[29] A. Tai,[6] J. Takahashi,[25] A. H. Tang,[15] D. Thein,[6] J. H. Thomas,[15] M. Thompson,[3]
V. Tikhomirov,[18] M. Tokarev,[9] M. B. Tonjes,[17] T. A. Trainor,[30] S. Trentalange,[6] R. E. Tribble,[27] V. Trofimov,[18] O. Tsai,[6]
T. Ullrich,[2] D. G. Underwood,[1] G. Van Buren,[2] A. M. VanderMolen,[17] I. M. Vasilevski,[10] A. N. Vasiliev,[22] S. E. Vigdor,[12]
S. A. Voloshin,[31] F. Wang,[23] H. Ward,[28] J.W. Watson,[14] R. Wells,[20] G. D. Westfall,[17] C. Whitten, Jr.,[6] H. Wieman,[15]
R. Willson,[20] S.W. Wissink,[12] R. Witt,[33] J. Wood,[6] N. Xu,[15] Z. Xu,[2] A. E. Yakutin,[22] E. Yamamoto,[15] J. Yang,[6] P. Yepes,[24]
V. I. Yurevich,[9] Y.V. Zanevski,[9] I. Zborovský,[9] H. Zhang,[33] W. M. Zhang,[14] R. Zoulkarneev,[10] and A. N. Zubarev[9]

(STAR Collaboration)

[1]*Argonne National Laboratory, Argonne, Illinois 60439*
[2]*Brookhaven National Laboratory, Upton, New York 11973*
[3]*University of Birmingham, Birmingham, United Kingdom*
[4]*University of California, Berkeley, California 94720*
[5]*University of California, Davis, California 95616*
[6]*University of California, Los Angeles, California 90095*
[7]*Carnegie Mellon University, Pittsburgh, Pennsylvania 15213*
[8]*Creighton University, Omaha, Nebraska 68178*

0031-9007/03/90(8)/082302(6)$20.00

[9]*Laboratory for High Energy (JINR), Dubna, Russia*
[10]*Particle Physics Laboratory (JINR), Dubna, Russia*
[11]*University of Frankfurt, Frankfurt, Germany*
[12]*Indiana University, Bloomington, Indiana 47408*
[13]*Institut de Recherches Subatomiques, Strasbourg, France*
[14]*Kent State University, Kent, Ohio 44242*
[15]*Lawrence Berkeley National Laboratory, Berkeley, California 94720*
[16]*Max-Planck-Institut fuer Physik, Munich, Germany*
[17]*Michigan State University, East Lansing, Michigan 48824*
[18]*Moscow Engineering Physics Institute, Moscow, Russia*
[19]*City College of New York, New York City, New York 10031*
[20]*The Ohio State University, Columbus, Ohio 43210*
[21]*Pennsylvania State University, University Park, Pennsylvania 16802*
[22]*Institute of High Energy Physics, Protvino, Russia*
[23]*Purdue University, West Lafayette, Indiana 47907*
[24]*Rice University, Houston, Texas 77251*
[25]*Universidade de Sao Paulo, Sao Paulo, Brazil*
[26]*SUBATECH, Nantes, France*
[27]*Texas A&M University, College Station, Texas 77843*
[28]*University of Texas, Austin, Texas 78712*
[29]*Warsaw University of Technology, Warsaw, Poland*
[30]*University of Washington, Seattle, Washington 98195*
[31]*Wayne State University, Detroit, Michigan 48201*
[32]*Institute of Particle Physics, CCNU (HZNU), Wuhan, 430079 China*
[33]*Yale University, New Haven, Connecticut 06520*

(Received 25 October 2002; published 26 February 2003)

Azimuthal correlations for large transverse momentum charged hadrons have been measured over a wide pseudorapidity range and full azimuth in Au + Au and $p + p$ collisions at $\sqrt{s_{NN}} = 200$ GeV. The small-angle correlations observed in $p + p$ collisions and at all centralities of Au + Au collisions are characteristic of hard-scattering processes previously observed in high-energy collisions. A strong back-to-back correlation exists for $p + p$ and peripheral Au + Au. In contrast, the back-to-back correlations are reduced considerably in the most central Au + Au collisions, indicating substantial interaction as the hard-scattered partons or their fragmentation products traverse the medium.

DOI: 10.1103/PhysRevLett.90.082302 PACS numbers: 25.75.–q

In collisions of heavy nuclei at high energies, a new state of matter consisting of deconfined quarks and gluons at high density is expected [1]. Large transverse momentum (p_T) partons in the high-density system result from the initial hard scattering of nucleon constituents. After a hard scattering, the parton fragments to create a high-energy cluster (jet) of particles. A high-momentum parton traversing a dense colored medium is predicted to experience substantial energy loss [2,3] and may be absorbed. Measurement of the parton fragmentation products after hard-scattering processes in nuclear collisions may reveal effects due to the interaction of high-p_T partons traversing the medium, thereby measuring the gluon density of the medium [4].

Hard-scattering processes have been established at high p_T in elementary collisions at high energy through the measurement of jets [5–7], back-to-back jets (dijets) [8], high-p_T single particles, and back-to-back correlations between high-p_T hadrons [9]. Jets have been shown to carry the momentum of the parent parton [10]. The jet cross sections and high-p_T single particle spectra are well described over a broad range of energies [11] in terms of the hadron's parton distributions, hard parton scattering treated by perturbative QCD, and subsequent fragmentation of the parton. In the absence of effects of the nuclear medium, the rate of hard processes should scale linearly with the number of binary nucleon-nucleon collisions. Recent results from the Relativistic Heavy-Ion Collider (RHIC), however, show a suppression of the single particle inclusive spectra of hadrons for $p_T > 2$ GeV/c in central Au + Au collisions, indicating substantial in-medium interactions [12,13].

In this Letter, we report measurements of two-hadron angular correlations at large transverse momentum for $p + p$ and Au + Au collisions at $\sqrt{s_{NN}} = 200$ GeV. These measurements provide the most direct evidence for production of jets in high-energy nucleus-nucleus collisions and allow first measurements, inaccessible in inclusive spectra, of the fate of back-to-back jets in the dense medium as a function of the size of the overlapping system. The results suggest significant interaction of hard-scattered partons (or their fragmentation products) in the medium, with a strong dependence on the geometry and distance of traversal.

The measurements were made using the STAR detector [14] at RHIC at Brookhaven National Laboratory. STAR is a large acceptance magnetic spectrometer, with a large time projection chamber (TPC) inside a 0.5 T solenoidal magnet. The TPC measures the trajectories of charged particles and determines the particle momenta. The TPC has full azimuthal coverage over a pseudorapidity range $|\eta| < 1.5$. STAR has excellent position and momentum resolution [the Gaussian width of the track curvature $k \propto 1/p_T$ is $\delta k/k = 0.005[p_T/(\mathrm{GeV}/c)] + 0.0076$], and, due to its vertexing capabilities, identifies many sources of secondary particles. The $p + p$ analysis uses $\approx 10 \times 10^6$ minimum bias $p + p$ events triggered on the coincidence of signals from scintillator annuli spanning $3.5 \leq |\eta| \leq 5.0$. The Au + Au analysis uses $\approx 1.7 \times 10^6$ minimum bias events and $\approx 1.5 \times 10^6$ top 10% central events.

Partons fragment into jets of hadrons in a cone around the direction of the original hard-scattered parton. The leading hadron in the jet tends to be most closely aligned with the original parton direction [15]. The large multiplicities in Au + Au collisions make full jet reconstruction impractical. Thus, we utilize two-particle azimuthal correlations of high-p_T charged hadrons [16] to identify jets on a statistical basis, with known sources of background correlations subtracted.

Events with at least one large transverse momentum hadron ($4 < p_T^{\mathrm{trig}} < 6$ or $3 < p_T^{\mathrm{trig}} < 4$ GeV/c), defined to be a *trigger* particle, are used in this analysis. For each of the trigger particles in the event, we increment the number $N(\Delta\phi, \Delta\eta)$ of *associated* tracks with $2\ \mathrm{GeV}/c < p_T < p_T^{\mathrm{trig}}$ as a function of their azimuthal ($\Delta\phi$) and pseudorapidity ($\Delta\eta$) separations from the trigger particle. We then construct an overall azimuthal pair distribution per trigger particle,

$$D(\Delta\phi) \equiv \frac{1}{N_{\mathrm{trigger}}} \frac{1}{\epsilon} \int d\Delta\eta N(\Delta\phi, \Delta\eta), \qquad (1)$$

where N_{trigger} is the observed number of tracks satisfying the trigger requirement. The efficiency ϵ for finding the associated particle is evaluated by embedding simulated tracks in real data. In order to have a high and constant tracking efficiency, the tracks are restricted to $|\eta| < 0.7$; hence, $|\Delta\eta| < 1.4$. The track reconstruction efficiency varies from 77% for the most central Au + Au collisions to 90% for the most peripheral Au + Au and $p + p$ collisions.

Identical analysis procedures are applied to the $p + p$ and Au + Au data. Displayed in Fig. 1 are the azimuthal distributions for same-sign and opposite-sign charged pairs from the (a) $p + p$ data and (b) minimum bias Au + Au data for $4 < p_T^{\mathrm{trig}} < 6$ GeV/c. The data are integrated over the relative pseudorapidity range $0 < |\Delta\eta| < 1.4$. Clear correlation peaks are observed near $\Delta\phi \sim 0$ and $\Delta\phi \sim \pi$ in the data. The opposite-sign correlations at small relative azimuth are larger than those of the same-sign particle pairs, while the sign has a negligible effect on the back-to-back correlations.

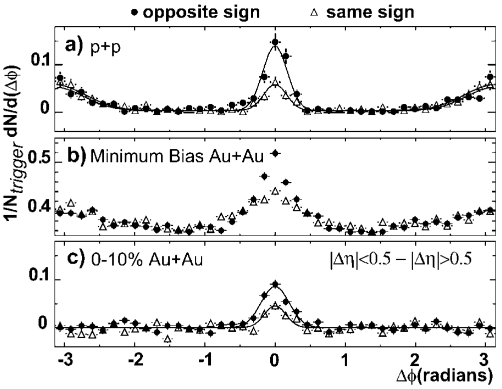

FIG. 1. Azimuthal distributions of same-sign and opposite-sign pairs for (a) $p + p$, (b) minimum bias Au + Au, and (c) background-subtracted central Au + Au collisions. All correlation functions require a trigger particle with $4 < p_T^{\mathrm{trig}} < 6$ GeV/c and associated particles with $2\ \mathrm{GeV}/c < p_T < p_T^{\mathrm{trig}}$. The curves are one or two Gaussian fits.

To isolate the jetlike correlations (localized in $\Delta\phi$, $\Delta\eta$) in central Au + Au collisions, the azimuthal distributions are measured for two regions, $|\Delta\eta| < 0.5$ and $0.5 < |\Delta\eta| < 1.4$ [16]. The difference between these two azimuthal distributions is displayed in Fig. 1(c) along with single Gaussian fits. Near $\Delta\phi = 0$, the azimuthal distributions from Au + Au and $p + p$ have similar shapes. For the opposite-sign [same-sign] azimuthal distributions, the Gaussian widths are $0.17 \pm 0.01(\mathrm{stat}) \pm 0.03(\mathrm{syst})$ $[0.16 \pm 0.02 \pm 0.03]$ rad for $p + p$ data and $0.20 \pm 0.02 \pm 0.03$ $[0.15 \pm 0.03 \pm 0.04]$ rad for the central Au + Au data. The systematic errors reflect the spread of values found for different choices of $\Delta\phi$ bin width. Within errors, the small-angle correlation widths are the same for $p + p$ and central Au + Au collisions.

The ratios of the opposite-sign to same-sign peak areas are $2.7 \pm 0.9(\mathrm{stat}) \pm 0.2(\mathrm{syst})$ for $p + p$ and $2.5 \pm 0.6 \pm 0.2$ for central Au + Au collisions. The preference for oppositely charged leading and next-to-leading hadrons [17] arises in jet fragmentation from dynamical charge correlations that originate from the formation of $q\bar{q}$ pairs along a string between two partons. The Hijing event generator, which utilizes the Lund string fragmentation scheme [18] incorporating these concepts, predicts a ratio of 2.6 ± 0.7 for the opposite-sign to same-sign correlation strengths. The agreement of this ratio with those measured suggests that the same jet production mechanism is responsible for the $\Delta\phi \approx 0$ correlation of high-p_T charged hadrons in $p + p$ and central Au + Au collisions.

The decay of resonances would also lead to small-angle azimuthal correlations, but could not explain the observed correlation of particles with the same charge sign and the strong back-to-back correlations of large p_T particles seen for $p + p$ collisions in Fig. 1(a). The latter correlations, indicative of dijet events [9], are removed from the central Au + Au sample by the subtraction in Fig. 1(c). A quantitative analysis of back-to-back jet survival in Au + Au requires the more detailed treatment of background correlations described below.

In addition to correlations due to jets, the two-particle azimuthal distributions in Au + Au exhibit a structure attributable to an elliptic flow anisotropy of single particle production relative to the reaction plane [16], $dN/d(\phi - \Phi_r) \propto 1 + 2v_2 \cos[2(\phi - \Phi_r)]$, where Φ_r is the reaction-plane angle determined event by event and v_2 is the elliptic flow parameter. This leads to a two-particle azimuthal distribution of the form $dN/d\Delta\phi = B[1 + 2v_2^2 \cos(2\Delta\phi)]$. Previous measurements [16] using several methods have shown that sizable v_2 values persist to high p_T. In this Letter, v_2 is determined using a reaction-plane method.

A simple reference model can be constructed by subdividing the $N(\Delta\phi, \Delta\eta)$ trigger-associated particle pairs into two classes: (1) pairs arising from a common partonic hard-scattering subprocess, where the measured correlation for pp events provides a suitable template for comparison and (2) pairs from all other high-p_T sources, including independent hard scatterings within the same event. Assuming that the only azimuthal correlation for class 2 pairs is that from elliptic flow, the model suggests a two-particle distribution,

$$D^{\text{model}} = D^{pp} + B[1 + 2v_2^2 \cos(2\Delta\phi)]. \tag{2}$$

The elliptic flow parameter (v_2) is measured independently in the same set of events and is taken to be constant for $p_T > 2$ GeV/c [16] (i.e., the same for trigger and associated particles). The parameter B, introduced as an estimate of the *a priori* unknown fraction of all pairs falling in class 2, is then determined by fitting the observed D^{AuAu} in the region $0.75 < |\Delta\phi| < 2.24$ rad, where the measured D^{pp} is close to zero.

In Fig. 2, the azimuthal distributions for $0 < |\Delta\eta| < 1.4$ in Au + Au collisions at various centralities are compared to Eq. (2) using the measured $p + p$ data. The centrality selection is constructed by subdividing the Au + Au minimum bias data sample into subsamples with different charged particle multiplicities within $|\eta| < 0.5$. The parameters v_2 and B are determined independently for each centrality bin and are listed in Table I. For all centralities, the azimuthal correlation near $\Delta\phi = 0$ is well described by Eq. (2). However, the back-to-back correlations are suppressed in Au + Au collisions compared to the expectation from Eq. (2), and the suppression is greater for more central collisions. The most central collisions show no indication of any back-to-back correlations beyond that expected from elliptic flow.

The ratio of the measured Au + Au correlation excess relative to the $p + p$ correlation is

$$I_{AA}(\Delta\phi_1, \Delta\phi_2) = \frac{\int_{\Delta\phi_1}^{\Delta\phi_2} d(\Delta\phi)\{D^{\text{AuAu}} - B[1 + 2v_2^2 \cos(2\Delta\phi)]\}}{\int_{\Delta\phi_1}^{\Delta\phi_2} d(\Delta\phi) D^{pp}}. \tag{3}$$

The ratio can be plotted as a function of the number of participating nucleons (N_{part}), deduced from the centrality bins as described in Ref. [13]. I_{AA} is measured for both the small-angle ($|\Delta\phi| < 0.75$ rad) and back-to-back ($|\Delta\phi| > 2.24$ rad) regions. The ratio should be unity if the hard-scattering component of Au + Au collisions is a superposition of $p + p$ collisions unaffected by the nuclear medium. These ratios are given in Fig. 3 for the trigger particle momentum ranges indicated. The asymmetric systematic errors are dominated by the +5%/−20% systematic uncertainty on v_2 due to the potential

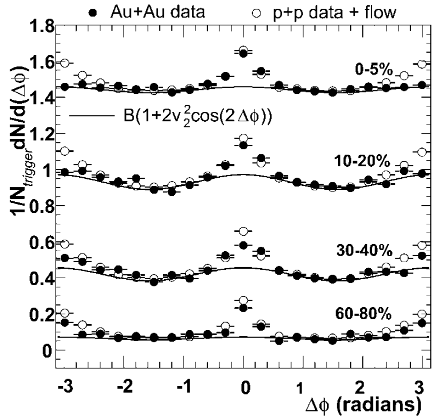

FIG. 2. Azimuthal distributions ($0 < |\Delta\eta| < 1.4$, $4 < p_T^{\text{trig}} < 6$ GeV/c) for Au + Au collisions (solid circles) compared to the expected distributions D^{model} from Eq. (2) (open circles). Also shown is the elliptic flow contribution for each centrality (solid curve).

TABLE I. Centrality, number of participants, v_2 ($2 < p_T < 6$ GeV/c), and normalization constant B. The errors on v_2 and B are statistical only, while the errors on the number of participants are systematic [13].

Centrality (%)	N_{part}	v_2	B
60–80	20 ± 6	0.24 ± 0.04	0.065 ± 0.003
40–60	61 ± 10	0.22 ± 0.01	0.231 ± 0.003
30–40	114 ± 13	0.21 ± 0.01	0.420 ± 0.005
20–30	165 ± 13	0.19 ± 0.01	0.633 ± 0.005
10–20	232 ± 11	0.15 ± 0.01	0.931 ± 0.006
5–10	298 ± 10	0.10 ± 0.01	1.187 ± 0.008
0–5	352 ± 7	0.07 ± 0.01	1.442 ± 0.003

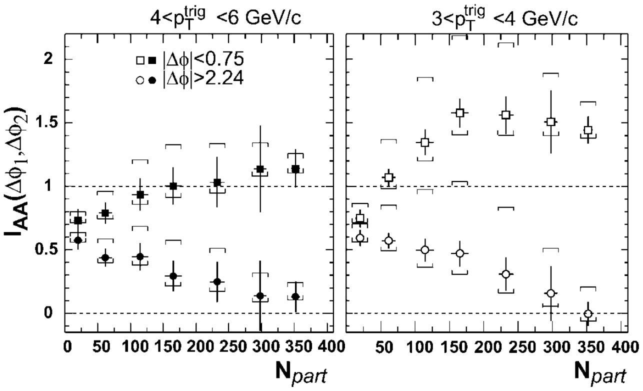

FIG. 3. Ratio of Au + Au and $p+p$ [Eq. (3)] for small-angle (squares, $|\Delta\phi| < 0.75$ rad) and back-to-back (circles, $|\Delta\phi| > 2.24$ rad) azimuthal regions versus number of participating nucleons for trigger particle intervals $4 < p_T^{trig} < 6$ GeV/c (solid) and $3 < p_T^{trig} < 4$ GeV/c (hollow). The horizontal bars indicate the dominant systematic error (highly correlated among points) from the uncertainty in v_2.

nonflow (including jet) contributions [19] as well as other sources of systematic uncertainty [16].

For the most peripheral bin (smallest N_{part}), both the small-angle and back-to-back correlation strengths are suppressed compared to the expectation from Eq. (2). This may be an indication of initial-state nuclear effects such as shadowing of parton distributions or scattering by multiple nucleons, or it may be indicative of energy loss in a dilute medium [20]. As N_{part} increases, the small-angle correlation strength increases, with a more pronounced increase for the trigger particles with lower p_T threshold. A large nonjet contribution to particle production above p_T^{trig} would dilute the jet related correlation signal and reduce this ratio. The back-to-back correlation strength, above background from elliptic flow, decreases with increasing N_{part} and is consistent with zero for the most central collisions. In the extreme case, if there were *no* elliptic flow for the 0%–5% most central collisions, $I_{AA}(2.24, \pi) = 0.4 \pm 0.1$ for $4 < p_T^{\text{trig}} < 6$ GeV/c, compared to $I_{AA}(2.24, \pi) = 0.1 \pm 0.1$ using the measured elliptic flow value. Therefore, an overestimation of the elliptic flow cannot explain the observed suppression of back-to-back correlations.

Analyses of fixed-target experiments [21] have suggested that the shape of the back-to-back dihadron azimuthal distribution is sensitive to the intrinsic parton transverse momentum k_T in the initial state. In proton-nucleus and nucleus-nucleus collisions, additional initial-state transverse momentum can be generated by multiple nucleon-nucleon interactions preceding a hard scattering [22–24]. To investigate whether this nuclear k_T can account for the observed deficit of back-to-back azimuthal correlations in central Au + Au collisions, we have carried out Pythia [18] simulations varying the Gaussian k_T parameter. A rather extreme change from the nominal value of $\sigma = 1$ GeV/c to 4 GeV/c introduced only a small effect, reducing the predicted $I_{AA}(2.24, \pi)$ by less than 20%. Experimental study of initial-state effects on the azimuthal correlations requires the measurement of $p(d)$ + Au collisions at RHIC energies.

In addition to the present data, two other striking effects have been observed at high p_T in nuclear collisions at RHIC: strong suppression of the inclusive hadron yield in central collisions [12,13] and large elliptic flow which saturates at $p_T > 3$ GeV/c [16]. These phenomena suggest a picture in which hadrons at $p_T >$ 3–4 GeV/c are primarily fragments of hard-scattered partons, and partons or their fragments are strongly scattered or absorbed in the nuclear medium. The observed hadrons therefore result preferentially from partons generated on the periphery of the reaction zone and heading outwards [25]. In this picture, the inclusive yield will be suppressed relative to the binary scaling expectation, and the strong position-momentum correlation required to explain the large elliptic flow [26] emerges naturally. Small-angle hadron correlations will have weak dependence on the size of the colliding system, whereas back-to-back correlations will exhibit strong suppression for a large system relative to a small one, both as observed.

In summary, STAR has measured azimuthal correlations for high-p_T charged particles over a large relative pseudorapidity range with full azimuthal angle coverage. Comparison of the opposite-sign and same-sign correlation strengths indicates that hard scattering and fragmentation are major sources of charged hadrons with $p_T > 4$ GeV/c in central Au + Au collisions. The azimuthal correlations in Au + Au collisions have been treated as the superposition of independently determined elliptic flow and individual hard parton scattering contributions, the latter measured in the STAR $p+p$ data. The most striking feature of the hard-scattering component is an increasing suppression of back-to-back relative to small-angle correlations with increasing centrality. These observations appear consistent with large energy loss in a system that is opaque to the propagation of high-momentum partons or their fragmentation products.

We thank the RHIC Operations Group and the RHIC Computing Facility at Brookhaven National Laboratory, and the National Energy Research Scientific Computing Center at Lawrence Berkeley National Laboratory for their support. This work was supported by the Division of Nuclear Physics and the Division of High-Energy Physics of the Office of Science of the U.S. Department of Energy, the United States National Science Foundation, the Bundesministerium fuer Bildung und Forschung of Germany, the Institut National de la Physique Nucleaire et de la Physique des Particules of France, the United Kingdom Engineering and Physical Sciences Research Council, Fundacao de Amparo a Pesquisa do Estado de

Sao Paulo, Brazil, the Russian Ministry of Science and Technology, and the Ministry of Education of China and the National Natural Science Foundation of China.

[1] See, for example, J.W. Harris and B. Müller, Annu. Rev. Nucl. Part. Sci. **46**, 71 (1996).
[2] M. Gyulassy and M. Plümer, Phys. Lett. B **243**, 432 (1990).
[3] X. N. Wang and M. Gyulassy, Phys. Rev. Lett. **68**, 1480 (1992).
[4] See, for example, R. Baier, D. Schiff, and B.G. Zakharov, Annu. Rev. Nucl. Part. Sci. **50**, 37 (2000).
[5] M. Banner *et al.*, Phys. Lett. B **118**, 203 (1982).
[6] G. Arnison *et al.*, Phys. Lett. B **123**, 115 (1983).
[7] F. Abe *et al.*, Phys. Rev. Lett. **62**, 613 (1989).
[8] F. Abe *et al.*, Phys. Rev. D **41**, 1722 (1990).
[9] G. Arnison *et al.*, Phys. Lett. B **118**, 173 (1982).
[10] F. Abe *et al.*, Phys. Rev. Lett. **65**, 968 (1990).
[11] T. Akesson *et al.*, Phys. Lett. B **123**, 133 (1983); J. A. Appel *et al.*, Phys. Lett. B **160**, 349 (1985); G. Arnison *et al.*, Phys. Lett. B **172**, 461 (1986); J. F. Owens, Rev. Mod. Phys. **59**, 465 (1987).
[12] K. Adcox *et al.*, Phys. Rev. Lett. **88**, 022301 (2002).
[13] C. Adler *et al.*, Phys. Rev. Lett. **89**, 202301 (2002).
[14] K. H. Ackermann *et al.*, Nucl. Instrum. Methods Phys. Res. (to be published).
[15] G. Arnison *et al.*, Phys. Lett. B **132**, 223 (1983).
[16] C. Adler *et al.*, Phys. Rev. Lett. **90**, 032301 (2003).
[17] P. Abreu *et al.*, Phys. Lett. B **407**, 174 (1997).
[18] T. Sjöstrand *et al.*, Comput. Phys. Commun. **135**, 238 (2001).
[19] C. Adler *et al.*, Phys. Rev. C **66**, 034904 (2002).
[20] F. Arleo, Phys. Lett. B **532**, 231 (2002); E. Wang and X. N. Wang, Phys. Rev. Lett. **89**, 162301 (2002).
[21] L. Apanasevich *et al.*, Phys. Rev. Lett. **81**, 2642 (1998).
[22] J.W. Cronin *et al.*, Phys. Rev. D **11**, 3105 (1975).
[23] M. D. Corcoran *et al.*, Phys. Lett. B **259**, 209 (1991).
[24] M. Lev and B. Petersson, Z. Phys. C **21**, 155 (1983).
[25] J. D. Bjorken, Report No. Fermilab-Pub-82/59-THY (1982).
[26] E.V. Shuryak, Phys. Rev. C **66**, 027902 (2002).